ORIGINAL PAPER

CrossMark

Poly(aminohippuric acid)–sodium dodecyl sulfate/functionalized graphene oxide nanocomposite for amplified electrochemical sensing of gallic acid

Mehdi Baghayeri[1] · Amirhassan Amiri[1] · Ehteram Hasheminejad[2] · Behnam Mahdavi[1]

Abstract

Gallic acid (GA), as a main phenolic acid, has been considered the main player on the human health, including the effects of reduction of cholesterol, depression of hypertension, anti-oxidation, anti-microbial, protection against cardiovascular disease and cancer. This study describes the development, electrochemical characterization and utilization of a novel functionalized graphene oxide/poly(p-aminohippuric acid)–sodium dodecyl sulfate nanocomposite modified glassy carbon electrode (APTS@GO/PPAH-SDS/GCE) for the electrocatalytic determination of GA. The synthesized nanocomposite was characterized by different techniques such as Fourier-transform infrared spectroscopy, thermo-gravimetric analysis and transmission electron microscopy. The electrochemical oxidation of GA was investigated by cyclic voltammetry, differential pulse voltammetry and amperometry. The modified electrode showed a potent and persistent electron mediating behavior followed by well-defined oxidation peak of GA and the linear range of 0.006–2000 $\mu mol\ L^{-1}$ with a detection limit of 1.7 $nmol\ L^{-1}$ for GA (S/N = 3) using amperometric method. Also, it was successfully used for the GA determination in the black tea and tab water as real samples. Additionally, this electrode exhibited good stability and reproducibility. The results imply that the APTS@GO/PPAH-SDS nanocomposite might be a promising candidate for practical applications in GA electrochemical detection.

Introduction

Determination of phenolic compounds has received much attention in recent years owing to their wide-ranging biological significance and potential application. Phenolic compounds are commonly presented in the plants and widely existing plant foodstuffs [1]. Gallic acid (GA) known as 3,4,5-trihydroxybenzoic acid ($C_6H_2(OH)_3COOH$) is one of the main phenolic components. It can be found in gallnuts, grapes, sumac, witch hazel, tea leaves, hops, and oak bark [2, 3] which has been widely used for the pharmaceutical and food industry due to its biological properties, anti-inflammatory antihistaminic and antitumor activities, scavenging of free radicals and protection against cardiovascular diseases involved [4]. Therefore, the quantitative determination of GA concentration in food, medicinal plants and human fluids is desirable for developing biology, pharmacological research and life science. In the past years, several techniques have been applied for the determination of GA due to its pharmacological importance [5–7]. Electrochemistry suggests quite attractive routine analysis capabilities, because such methods are sensitive, inexpensive, simple, fast and can be performed with miniaturized, portable instrumentation [8–10]. Several electrochemical methods have been developed for GA determination in different matrices, especially in tea and wine samples [1, 11, 12]. In actual, in the electrochemical methods, determination of GA is based on its electrochemical oxidation signal. The direct electrochemical oxidation of GA is possible, but requires high overpotentials about 1000 mV at bare GCE electrodes. These high overpotentials result in electrode fouling, poor reproducibility, low selectivity and poor sensitivity, and thus this technique is rarely employed analytically [13]. A promising approach to overcome these difficulties is application of the various

✉ Mehdi Baghayeri
m.baghayeri@hsu.ac.ir

[1] Department of Chemistry, Faculty of Science, Hakim Sabzevari University, P.O. Box 397, Sabzevar, Iran

[2] Young Researchers and Elite Club, Sabzevar Branch, Islamic Azad University, Sabzevar, Iran

electron mediators such as carbon nanotubes, conductive polymers and metal nanoparticles to modify electrodes for lowering the overpotential and enhancement of current [14, 15]. In this case, immobilization of the electron mediator at the surface of modified electrode has a significant role in stability and reproducibility of its electrochemical responses [16]. The ability of anions to incorporate into the conducting polymer matrix as doping ions offers a fast, and simple method of immobilization of electron mediators and preparing chemically modified electrodes [17].

In recent times, the electrodes modified with graphene-metal nanoparticles composite have attracted wide attention in many fields owing to their high electron conductivity and well biocompatibility [18–20]. Graphene, a one-atom-thick planar sheet of sp^2-bonded carbon atoms, has attracted great regard since it was first discovered in 2004 [21]. Because of its unique properties, such as large surface area, high electrical conductivity, rapid heterogeneous electron transfers and good electrocatalytic activity [22], graphene has been used as a perfect electrode material in cells [23, 24], supercapacitors [25], field-effect transistors [26] and chem/bio-sensors [27, 28]. Now, the techniques for preparation of graphene mainly include mechanical exfoliation [21], chemical vapor deposition (CVD) [29], epitaxial growth [30] and chemical or thermal reduction [31]. Most of graphene employed in electrochemistry is prepared from the reduction of graphene oxide (GO), and typically has functional groups such as carboxyl, hydroxyl and amine which are favorable for adsorbing heavy metal ions [32]. On the other hand, polymer-modified electrodes have many advantages when used in electrochemical approaches of analysis [33–35] and electropolymerization is a successful technique for the immobilization of polymers [36, 37] which allows the control of film thickness and other characteristics for polymers. Such modified electrodes include high selectivity and sensitivity, homogeneity of electrochemical deposition, strong polymer adherence, as well as chemical stability of film [38–41]. Immobilization of nanoparticles on electrode surface, e.g. glassy carbon electrode (GCE) has been significantly improved [34–38] by electropolymerization of suitable monomers such as aminohippuric acid or *para*-aminohippuric acid (PAH), a derivative of hippuric acid, which has been used as complexing agent with various metal ions [42]. Also, this reagent has a –NH_2 functional group that can be attached to the electrode surface to prepare a selective sorbent/modifier. Hence, in this work, PPAH was used to enhance the performance features of the sensor and to efficiently immobilize aminopropyltrimethoxysilane@graphene oxide (APTS@GO) onto the electrode surfaces. Indeed, the APTS@GO/PPAH-SDS/GCE selected to investigate the voltammetric behavior of GA and also improve the GA detection at low concentration levels by a simple, rapid, and direct detection method. The impact of loaded PPAH value was also studied on the

electrochemical oxidation of GA. In addition, the reproducibility and stability of as-fabricated electrode was investigated and the electrode was also employed to analyze the GA at real samples.

Materials and methods

Reagents

Potassium chloride ($> 98\%$), sodium dodecyl sulfate (SDS) ($> 99\%$), gallic acid and *para*-aminohippuric acid (PAH) were purchased from Sigma-Aldrich. Ethanol, toluene, graphene oxide and 3-aminopropyltrimethoxysilane (APTS) were purchased from Merck. Phosphate buffer was prepared by mixing the stock solutions of 0.1 M NaH_2PO_4 and 0.1 M Na_2HPO_4 and then, adjusting the pH with H_3PO_4 (from Merck) or NaOH (from Merck). The GA solution was prepared by 0.1 M phosphate buffer (pH 7.0). The stock solution was stable when stored in a refrigerator at 4 °C for 1 month. All other chemicals (purchased from Merck) were of analytical grade and were used as received without any purification process.

Synthesis of APTS@GO

Graphene oxide was synthesized by Hummers method [43] and then, 1000 mg of graphene oxide was adequately dispersed in 250 ml toluene by using an ultrasonic probe. 3.0 ml of 3-aminopropyltrimethoxysilane (APTS) was added to the graphene oxide dispersion, and refluxed for 24 h under a nitrogen atmosphere. The obtained graphene nanosheets (named APTS@GO) were washed with toluene to remove excess/non-reacted APTS. Toluene washing was carried out four times and then ethanol was used for the final washing. The black cake of APTS@GO was dried in an oven at 70 °C [44].

Apparatus and instrumentations

Cyclic voltammetry measurements were carried out on a Metrohm (797 VA Computrace, Switzerland) controlled by personal computer. An Ag|AgCl|KCl (3 M) as reference electrode and a platinum wire as auxiliary electrode were used. Autolab electrochemistry instruments (Autolab, Eco Chemie, Netherlands) was applied for amperometry measurements. A glassy carbon electrode (Azar electrode Co., Urmia, Iran, with a geometrical area of 0.0314 cm^2), bare or modified, was used as working electrode. FT-IR spectra were recorded on a Bruker Tensor 27 spectrometer (Bruker, karlsrohe, Germany). All experiments were performed at room temperature (25 ± 2 °C). X-Ray diffraction (XRD, Rigaku Corporation, Tokyo, Japan) patterns were obtained

at room temperature on a Riga kuD/Max-2550 powder diffractometer with a scan rate of $5°$ min^{-1} and recorded in 2θ range of 10–70°. Transmission electron microscopy (TEM), was performed on a CM1 electron microscope at an accelerating voltage of 120 kV, Philips, Netherland) was used to obtain information about the morphology of nanocomposite. Thermo-gravimetric analysis (TGA) of prepared adsorbents was investigated using the LENSES STAPT-1000 calorimeter (Germany) by scanning up to 800 °C with the heating rate of 10 °C min^{-1}. Electrolyte solutions were deoxygenated by purging pure nitrogen (99.99%) for 10 min prior to electrochemical experiments. All measurements were carried out under a nitrogen atmosphere.

Preparation of the modified electrodes

Before modification, GCE was polished with a polishing cloth and alumina slurry. Then, GCE was rinsed with dilute nitric acid, ethanol and distilled water in an ultrasonic bath and finally, it was electrochemically treated by potential cycling between − 1.0 and + 1.0 V in 0.25 mol L^{-1} H_2SO_4 solution until a steady state cycle was reached.

The electropolymerization of PAH on GCE was done by continuous potential cycling for 20 cycles in the range of − 0.1 to + 0.8 V vs. Ag|AgCl (3 M KCl) at a scan rate of 50 mV s^{-1} in 0.1 M KCl containing 1.0×10^{-3} M PAH and 1.0×10^{-3} M SDS. The PPAH-SDS/GCE was then rinsed and dried at ambient conditions. Next, 6.0 μL of APTS@GO ethanol solution (1.0 mg mL^{-1}) was casted on the surface of PPAH-SDS/GCE and dried in air and finally, the APTS@GO/PPAH-SDS/GCE was obtained.

Results and discussion

Characterization of materials

The products were characterized by FTIR, TEM, TGA and the elemental analysis, respectively. To know about the nature of GO surface modification, the FT-IR transmittance patterns of APTS@GO (curve a) along with GO-COOH sample (curve b) are shown in Fig. 1A. As can be seen, FTIR spectrum of GO exhibits the characteristic peaks at ~ 805 cm^{-1} (=C–H bending), ~ 1386 cm^{-1} (C–C stretching, C–H bending and O–H deformation), ~ 1626 cm^{-1} (C–C stretching), ~ 1722 cm^{-1} (C=O stretching vibration of the carboxylic acid), ~ 2873 cm^{-1} (O–H stretching vibration of the carboxylic acid), ~ 2918 cm^{-1} (C–H stretching) and ~ 3438 cm^{-1} (O–H stretching vibration of the phenols, alcohols and absorbed water). The FTIR spectrum of APTS@GO shows the sharper bands and characteristic peaks at ~ 1243 cm^{-1} (Si–CH$_2$ stretching), ~ 1364 cm^{-1} (C–N stretching), ~ 1661 cm^{-1} (N–H bending), ~ 3046 cm^{-1} (C–H stretching vibration of APTS aliphatic section) and ~ 3422 cm^{-1} (N–H stretching and its shoulder) in addition to the characteristic peaks of GO.

The morphology of APTS@GO was characterized by TEM. The obtained TEM images show a few layered structures for the GO. As can be seen, the transparent sheets are flake-like with wrinkles (Fig. 1B).

TGA/DTA result of an APTS@GO sample in N_2 atmosphere contains three major mass losses as shown in Fig. 1C. First stage is related to the loss of moisture with 4.7% weight reduction, the second mass loss stage is in the range of 260–400 °C with 14% weight reduction corresponding to the removal of oxygen functional groups and the third stage at the range of 430–550 °C with 25% weight loosing is due to the removal of APTS groups attached on the surface of GO by chemical bonds. This result showed the synthesis of the APTS@GO with the minimum amount of decrease in the oxygen functional groups which leads to loading of 1.0 mmol APTS on the 1.0 g GO (1.0 mmol g^{-1} APTS@GO).

The CHN elemental analysis of APTS@GO based on the presence of nitrogen well confirmed the high loading of APTS on the GO sheets. In addition, based on the total presence of carbon, hydrogen and nitrogen, one more again it was confirmed that the mentioned synthetic method is followed with the minimum reduction of oxygen functional groups.

In this work for preparation of polymer, the electrochemical polymerization of monomer was applied and performed by cyclic voltammetry (CV) at the GCE surface in the presence of SDS. It is noteworthy that the reason of using SDS in this work was the increase of polymerization rate and facilitating the polymer growth. The consecutive cyclic voltammograms recorded during the electropolymerization of PAH were shown in Fig. 2. Multiple cyclic voltammograms for the repeated scanning electropolymerization of PAH are observed. During the first positive scan, two single oxidation peaks are observed at about + 0.14 and + 1.13 V vs. Ag|AgCl, respectively, which corresponds to the irreversible behavior of monomer at the bare GCE surface and any distinct reversible cathodic peak is not appeared during the reverse scan. It is obvious that the peaks height related to the monomer oxidation decreases during the next cyclic voltammograms. In addition, the new oxidation and reduction peaks are evolved at about + 0.43 and + 0.34 V vs. Ag|AgCl, respectively, related to the polymer. In fact, upon the potential repeated scanning, an electroactive polymer film quickly grows on the GCE which is accompanied with the increase of current intensity in successive cycles. These results evidence the presence of PPAH on the surface of modified electrode.

Fig. 1 **A** FT-IR spectra of APTS@GO (curve a) and GO-COOH (curve b), **B** TEM images of APTS@GO, **C** TGA spectrum of APTS@GO
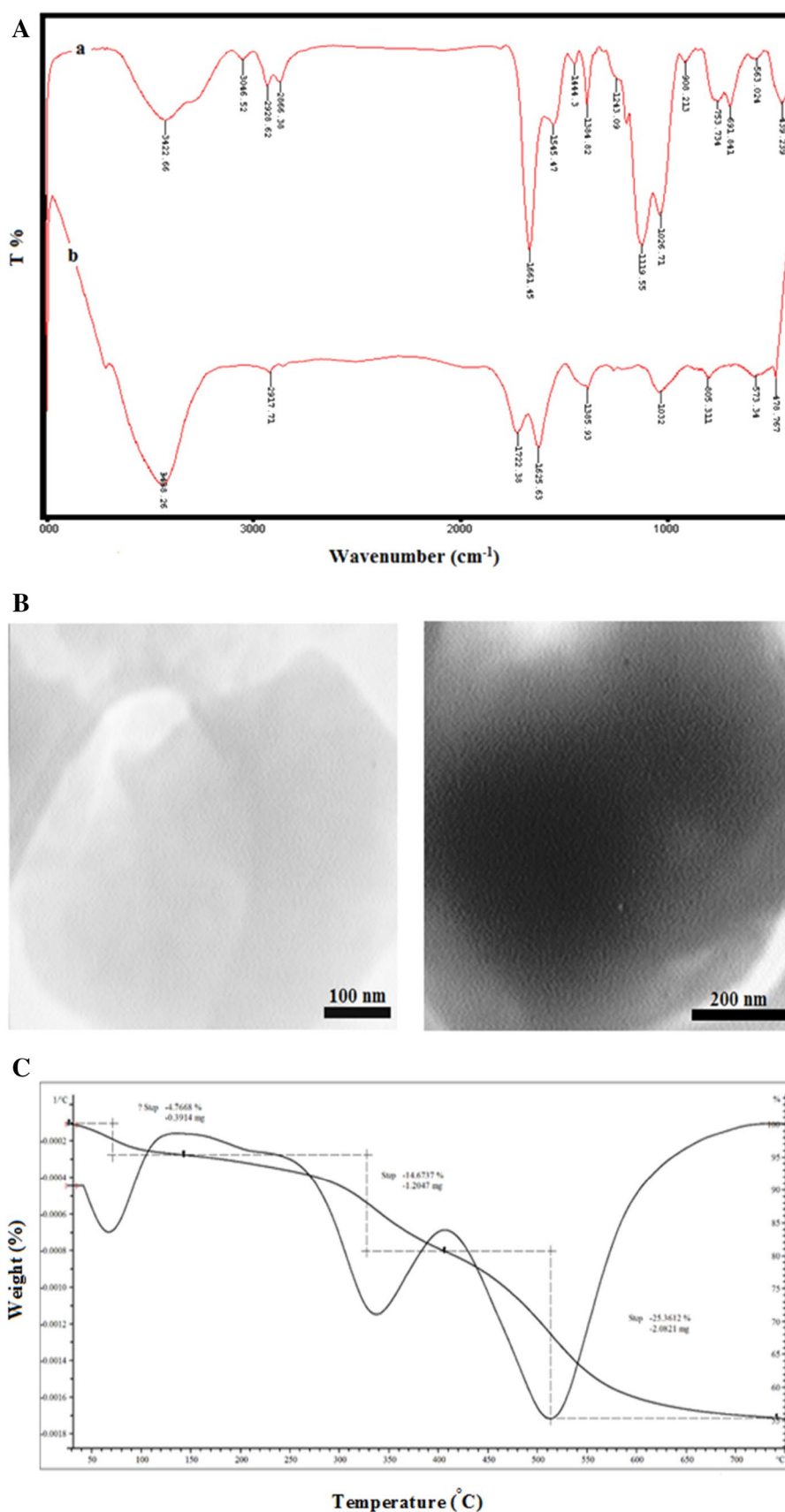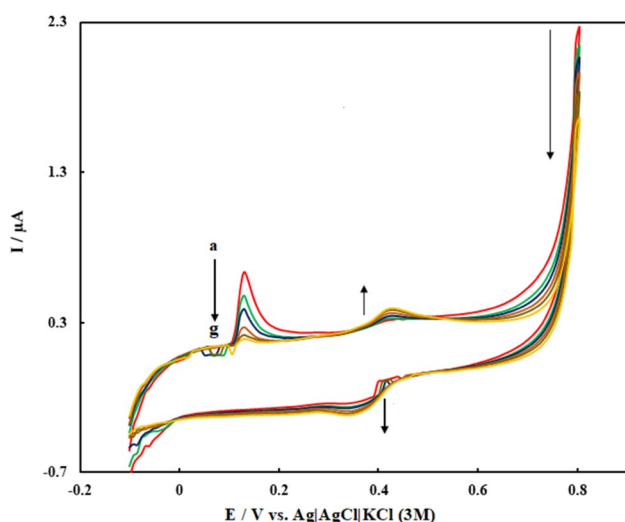
Fig. 2 Electropolymerization of 1.0×10^{-3} M PAH monomer in 0.1 M KCl solution containing 1.0×10^{-3} M SDS at scan rate of 50 mV s^{-1} in the cycle of **a** 1st, **b** 4th, **c** 8th, **d** 12th, **e** 15th and **f** 20th. The arrows indicate the trends of current intensity during the cyclic voltammetric experiments

Study of the electrochemical behavior of GA

To study the electrocatalytic activity at the surface of different electrodes, electrochemical oxidation of GA was presented in 0.1 M phosphate buffer solution (PBS, pH 7.0) (Fig. 3). At the bare GCE and in the absence of GA, no peak was observed (curve a). At the bare GCE and in the presence of 2.28 µmol L^{-1} GA (curve b), the peak of GA was not clearly appearing in the studied potential window. At the APTS@GO/PPAH-SDS/GCE and in the presence of 2.28 µmol L^{-1} GA (curve c), GA showed two oxidation

peaks at the potentials of 0.57 and 0.88 V which is consistent with that reported in the literature [45, 46] and peak current improved significantly. Compared with bare GCE, APTS@ GO/PPAH-SDS/GCE enhanced the kinetics of the electrochemical process as an efficient promoter demonstrating that the proposed sensor can be applied for the detection of GA. The good catalytic activity of APTS@GO/PPAH-SDS/GCE can be attributed to the synergic effect of APTS@GO and PPAH which leads to the excellent properties such as high specific surface area and electrical conductivity. In fact, the attachment of APTS@GO on PPAH strongly increases the rate of electron transfer on this treated surface.

Electrode response toward GA electrooxidation depends on the amount of loaded PPAH on the modified electrode. Hence, the loading PPAH (performed under different number of cycles) was investigated at the surface of electrode. Figure 4 shows the typical linear sweep voltammograms recorded for GA during the electropolymerization of PAH on GCE by different cycle number. As can be observed, the peak current of GA increases with increasing the cycle number up to 20 cycles due to the increment in the amount of loaded PPAH. Based on this, 20 cycles are enough to saturate the electrode surface by loaded PPAH that enhances the GA oxidation process. So, 20 cycles were selected for further studies.

Scan rate is one of the parameters that significantly affect the electrooxidation of various compounds. Thus, the scan rate study was done using cyclic voltammetry to evaluate whether the electrooxidation process of GA on modified electrode is surface or diffusion controlled. Figure 5 shows the CVs of APTS@GO/PPAH-SDS/GCE in 0.1 M PBS (pH 7.0) containing 50.0 µM GA with different potential scan
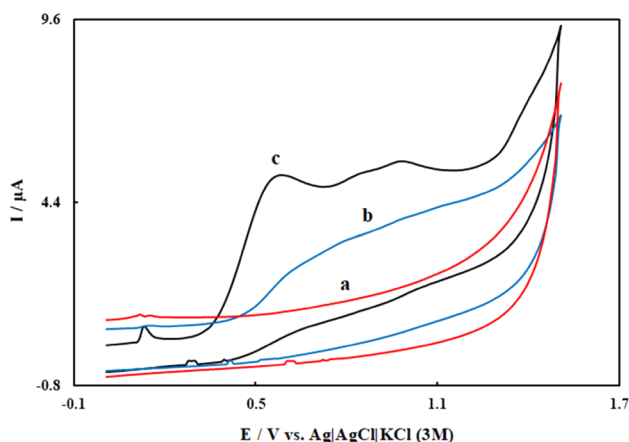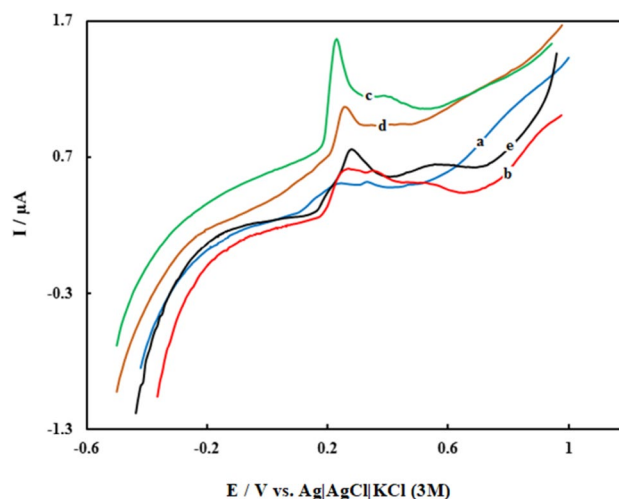

Fig. 3 Cyclic voltammograms on the bare GCE (**a, b**) and APTS@ GO/PPAH-SDS/GCE (**c**) in 0.1 M PBS (pH 7.0) in the absence (**a**) and presence of 2.28 µmol L^{-1} GA (**b, c**). Scan rate 50 mV s^{-1}

Fig. 4 Linear sweep voltammograms of 2.28 µM GA in 0.1 M PBS (pH 7.0) on the surface of APTS@GO/PPAH-SDS/GCE at different cycle numbers for loading the PPAH: **a** 5, **b** 10, **c** 20, **d** 30 and **e** 40 cycles
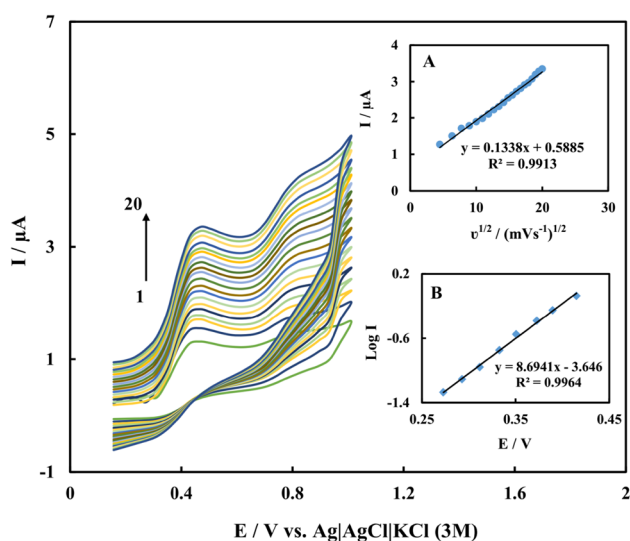
Fig. 5 Cyclic voltammograms of 2.28 μM GA in 0.1 M PBS (pH 7.0) on the surface of APTS@GO/PPAH-SDS/GCE at different scan rates: (1) 20, (2) 40, (3) 60, (4) 80, (5) 100, (6) 120, (7) 140, (8) 160, (9) 180, (10) 200, (11) 220, (12) 240, (13) 260, (14) 280, (15) 300, (16) 320, (17) 340, (18) 360, (19) 380 and (20) 400 mV s^{-1}. Inset A: plot of the anodic peak current vs. the potential scan rate. Inset B: Tafel plot for APTS@GO/PPAH-SDS/GCE in in 0.1 M PBS (pH 7.0) with a scan rate of 20 mV s^{-1} in the presence of 2.28 μM GA

rates at the range of 20–400 mV s^{-1}. As shown in the inset of Fig. 5, a linear plot of peak current vs. $v^{1/2}$ was obtained (described by the equation: $I_p = 0.1338\, v$ (mV s^{-1}) $+ 0.5885$ (μA), $R^2 = 0.9913$) proposing that the oxidation of GA is a diffusion-controlled process. To obtain further information on the rate determining step, a Tafel plot was obtained for the GA at a surface of modified electrode using the data derived from the raising part of the current–voltage curve (Fig. 6). The slope of the Tafel plot is equal to $n(1-\alpha)F/2.3\,RT$ which comes up to 8.6941 V decade^{-1}. We obtained $n\alpha$ as 0.486. Assuming $n = 1$, then $\alpha = 0.486$.

Determination of GA

To study the electrochemical analytical behaviors of modified electrode, electrooxidation of various concentrations of GA was carried out by CV and DPV. Figure 6 shows the CVs of the APTS@GO/PPAH-SDS/GCE in 0.1 M PBS (pH 7.0) containing a number of GA concentrations from 5 to 60 μM. As shown, by increasing the concentration of GA, the anodic peak current of GA is enhanced suggesting the excellent electrocatalytic activity of APTS@GO/PPAH-SDS. This phenomenon also demonstrated that APTS@GO/PPAH-SDS film was successfully immobilized on the GCE surface.

Since CV was not sensitive for the determination of low contents of compounds, DPV studies were performed. Figure 7 shows the DPV response of modified electrode to GA
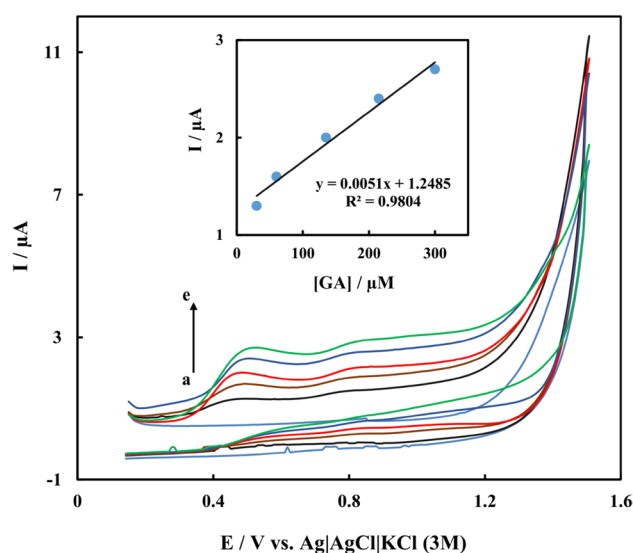

Fig. 6 Cyclic voltammograms of APTS@GO/PPAH-SDS/GCE in the presence of various concentrations of GA: 30 (**a**), 60 (**b**), 135 (**c**), 215 (**d**) and 300 μM (**e**) in 0.1 M PBS (pH 7.0) at the scan rate of 100 mV s^{-1}. Inset: plot of electrocatalytic peak current vs. concentration of GA

in 0.1 M PBS (pH 7.0). As can be seen in the inset of Fig. 7, the oxidation current increased with the gradual increase of GA concentration from 0.05 to 70 μM. The linear range equation was $I_p = 0.0093$ [GA] (μM) $+ 0.6748$ (μA) with $R^2 = 0.9723$.

To access to the high sensitivity and low detection limit for GA, the amperometry technique was used under optimum conditions of the fabricated electrochemical sensor. Figure 8 shows the amperometric response of modified
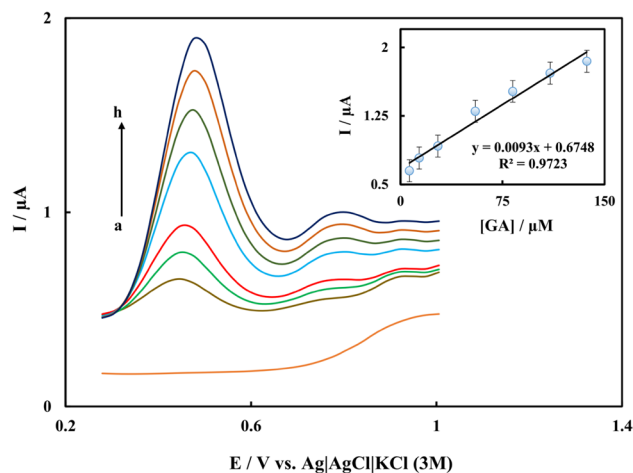

Fig. 7 Differential pulse voltammograms of APTS@GO/PPAH-SDS/GCE in the presence of various concentrations of GA: 0 (**a**), 6.6 (**b**), 13.75 (**c**), 27.5 (**d**), 55 (**e**), 82.5 (**f**), 110 (**g**) and 137 μM (**h**) in 0.1 M PBS (pH 7.0). Inset: plot of electrocatalytic peak current vs. concentration of GA
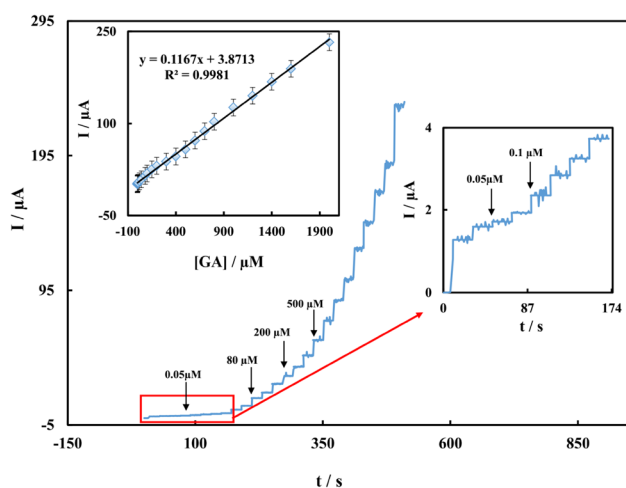
Fig. 8 Typical amperometric response of the sensor toward successive injections of GA with different concentrations (from 0.006 to 2000 µM) into the stirred solution of 0.1 M PBS (pH 7.0) at the applied potential of +0.6 V. Inset shows the calibration curve for the determination of GA

electrode toward GA in 0.1 M PBS (pH 7.0) at an applied potential of +0.6 V. As can be seen in the inset of Fig. 8, the oxidation current increased with the gradual increase of GA concentration from 0.006 to 2000 µM. The linear range equation was $I_p = 0.1167$ [GA] (µM) + 3.8713 (µA) with $R^2 = 0.9981$. The detection limit was estimated to be 1.7 nmol L^{-1} (S/N = 3). The proper wide linear range and low detection limit can be attributed to the synergetic effect of PPAH and APTS@GO in which PPAH provides a large specific surface area to immobilize APTS@GO (as an accelerator of the electron transfer on the electrode surface).

Reproducibility, stability and anti-interference property of the sensor

In the case of stability, the sensor showed a good and acceptable stability with a loss of only 13% in current response after 2 weeks. The reproducibility and precision of the proposed sensor were assessed by repeating the detection of a

GA certain concentration. The reproducibility was examined for five identically made electrodes with a relative standard deviation (RSD) of 5.1% while for 10 measurements by the same electrodes (performed upon the addition of 5.0 µM GA in 0.1 M PBS (pH 7.0) with RSD of 7.4% demonstrating an excellent reproducibility.

A number of oxidizable interfering species could co-exist with GA in many samples. Therefore, it is necessary to investigate whether such species could generate the current responses comparable to that of GA. The interference caused by various foreign species on the determination of 5.0 µM GA was studied and the resulting data were summarized in Table 1. The tolerable concentration ratios with respect to GA were more than 50.0 for K$^+$, F$^-$, Mg^{2+}, Ca^{2+} and 10.0 for glycline, glutamic acid, lysine, ethanol, ascorbic acid, dopamine, uric acid, catechinic acid, anthocyanin and also 1.0 for caffeic acid, respectively.

Analysis of the real samples

The proposed sensor was applied to determine GA in black tea and tab water samples. The determination of real samples was implemented by standard addition method in the similar conditions and the attained results are listed in Table 2. The results reveal that the fabricated sensor can be used to determine the GA in the routine real samples powerfully.

Table 2 Results of the GA detection in the real samples ($n = 5$)

Sample	Added (mg L^{-1})	Found (mg L^{-1})	Recovery (%)
Black tea	0.0	1.7	
	30.0	32 ± 0.05	106.6
	50.0	52.5 ± 0.04	102.5
	70.0	72 ± 0.07	102.8
	100.0	104 ± 0.05	104
Tab water	0.0	0.0	
	20.0	20.7 ± 0.03	103.5
	40.0	39.4 ± 0.04	98.5
	60.0	60.6 ± 0.07	101

Table 1 The effect of various substances on the determination of GA

Substance[a]	Amount (µM)	Relative error (%)	Substance[a]	Amount (mg L^{-1})	Relative error (%)
K$^+$	250.0	+2.5	Ethanol	50.0	2.2
F$^-$	250.0	−1	Ascorbic acid	50.0	+10
Mg^{2+}	250.0	−5.2	Dopamine	50.0	+8
Ca^{2+}	250.0	−4.6	Uric acid	50.0	2.1
Glycline	50.0	−7.5	Catechinic acid	50.0	−2.3
Glutamic acid	50.0	−4	Anthocyanin	50.0	−5.1
Lysine	50.0	+5	Caffeic acid	50.0	+3

[a]Added to the 5.0 µM GA

Conclusions

For the first time, a novel electrochemical sensor based on the APTS@GO/PPAH-SDS nanocomposite modified GCE was developed and successfully applied for the determination of GA. The use of functionalized graphene oxide along with PPAH on the electrode surface and the synergistic effect between them greatly improved the sensitivity of as-fabricated sensor. The developed sensor showed a good and acceptable reproducibility and stability for determination of GA. Most importantly, the lowest detectable concentration of GA was calculated to be 1.7 nmol L^{-1}. In addition, the analysis of GA in black tea and tab water samples proved the applicability of the sensor in the detection of GA in real samples. Finally, it can be concluded that the established method is easy to run, simple, fast, and accurate with a good analytical achievement.

Compliance with ethical standards

Conflict of interest The authors declare that they have no conflict of interest.

References

1. Z. Liang, H. Zhai, Z. Chen, H. Wang, S. Wang, Q. Zhou, X. Huang, Sens. Actuators B **224**, 915 (2016)
2. D. Rajalakshmi, S. Marasimhan, in *Food antioxidants: Sources and methods of evaluation*, ed. by D.L. By, S.S. Madhavi, D.K. Deshpande, Salunkhe (Marcel Dekker, New York, 1996), p. 65
3. B. Boye, E. Brillas, A. Buso, C. Farnia, C. Flox, M. Giomo, G. Sandona, Electrochim. Acta **52**, 256 (2006)
4. I. Mudnic, D. Modun, V. Rastija, J. Vukovic, I. Brizic, V. Katalinic, M. Kozina, B. Medic-Saric, M. Boban, Food Chem. **119**, 1205 (2010)
5. R. Jimenez-Prieto, M. Silva, D. Perez-Bendito, Anal. Chim. Acta **321**, 53 (1996)
6. S. Shahrzad, I. Bitsch, J. Chromatogr. B Biomed. Sci. Appl. **705**, 87 (1998)
7. Y. Zuo, H. Chen, Y. Deng, Talanta **57**, 307 (2002)
8. A. Mohadesi, M.A. Taher, Sens. Actuators B **123**, 733 (2007)
9. M. Baghayeri, A. Amiri, Z. Alizadeh, H. Veisi, E. Hasheminejad, J. Electroanal. Chem. **810**, 69 (2018)
10. M. Baghayeri, H. Veisi, M. Ghanei-Motlagh, Sens. Actuators B **249**, 321 (2017)
11. J. Tashkhourian, S.F. Nami-Ana, Mater. Sci. Eng. C **52**, 103 (2015)
12. J.H. Luo, B.L. Li, N.B. Li, H.Q. Luo, Sens. Actuators B **186**, 84 (2013)
13. M. Baghayeri, M. Namadchian, Electrochim. Acta **108**, 22 (2013)
14. M. Baghayeri, E.N. Zare, M. Namadchian, Sens. Actuators B **188**, 227 (2013)
15. M. Baghayeri, H. Veisi, Biosens. Bioelectron. **74**, 190 (2015)
16. M. Baghayeri, Sens. Actuators B **240**, 255 (2017)
17. M. Baghayeri, E.N. Zare, M.M. Lakouraj, Biosens. Bioelectron. **55**, 259 (2014)
18. F.Y. Kong, S.X. Gu, W.W. Li, T.T. Chen, Q. Xu, W. Wang, Biosens. Bioelectron. **56**, 77 (2014)
19. L. Zhu, L. Xu, B. Huang, N. Jia, L. Tan, S. Yao, Electrochim. Acta **115**, 471 (2014)
20. A. Safavi, R. Ahmadi, F.A. Mahyari, M. Tohidi, Sens. Actuators B **207**, 668 (2015)
21. K.S. Novoselov, A.K. Geim, S.V. Morozov, D. Jiang, Y. Zhang, S.V. Dubonos, I.V. Grigorieva, A.A. Firsov, Science **306**, 666 (2004)
22. S. Stankovich, D.A. Dikin, G.H.B. Dommett, K.M. Kohlhaas, E.J. Zimney, E.A. Stach, R.D. Piner, S.T. Nguyen, R.S. Ruoff, Nature **442**, 282 (2006)
23. C.T. Hsieh, Y.Y. Liu, A.K. Roy, Electrochim. Acta **64**, 205 (2012)
24. K. Ji, G. Chang, M. Oyama, X.Z. Shang, X. Liu, Y.B. He, Electrochim. Acta **85**, 84 (2012)
25. K. Zhang, L.L. Zhang, X.S. Zhao, J.S. Wu, Chem. Mater. **22**, 1392 (2010)
26. Y.Q. Wu, Y.M. Lin, A.A. Bol, K.A. Jenkins, F.N. Xia, D.B. Farmer, Y. Zhu, P. Avouris, Nature **472**, 74 (2011)
27. Y.J. Guo, S.J. Guo, J.T. Ren, Y.M. Zhai, S.J. Dong, E.K. Wang, ACS Nano **4**, 4001 (2010)
28. X. Yang, C.L. Chen, J.X. Li, G.X. Zhao, X.M. Ren, X.K. Wang, RSC Adv. **2**, 8821 (2012)
29. X.B. Wang, H.J. You, F.M. Liu, M.J. Li, L. Wan, S.Q. Li, Q. Li, Y. Xu, R. Tian, Z.Y. Yu, D. Xiang, J. Cheng, Chem. Vap. Depos. **15**, 53 (2009)
30. C. Berger, Z.M. Song, T.B. Li, X.B. Li, A.Y. Ogbazghi, R. Feng, Z.T. Dai, A.N. Marchenkov, E.H. Conrad, P.N. First, W.A. de Heer, J. Phys. Chem. B **108**, 19912 (2004)
31. S. Stankovich, D.A. Dikin, R.D. Piner, K.A. Kohlhaas, A. Kleinhammes, Y.Y. Jia, Y. Wu, S.T. Nguyen, R.S. Ruoff, Carbon **45**, 1558 (2007)
32. D. Du, J. Liu, X.Y. Zhang, X.L. Cui, Y.H. Lin, J. Mater. Chem. **21**, 8032 (2011)
33. N. Chauhan, J. Narang, C.S. Pundir, Biosens. Bioelectron. **29**, 82 (2011)
34. H.B. Li, J. Li, Q. Xu, X.Y. Hu, Anal. Chem. **83**, 9681 (2011)
35. L.T. Wang, Y. Zhang, Y.L. Du, D.B. Lu, Y.Z. Zhang, C.M. Wang, J. Solid State Chem. **16**, 1323 (2012)
36. M. Sen, U. Tamer, N.O. Pekmez, J. Solid State Chem. **16**, 457 (2012)
37. F.Y. Zhang, Z.H. Wang, Y.Z. Zhang, Z.X. Zheng, C.M. Wang, Y.L. Du, W.C. Ye, Talanta **93**, 320 (2012)
38. P.H. Yang, W.Z. Wei, L. Yang, Microchim. Acta **157**, 229 (2007)
39. G.J. Yang, J.K. Yan, F. Qi, C. Sun, Electroanalysis **22**, 2729 (2010)
40. S.J. Guo, Q.Q. Zhu, B.C. Yang, J. Wang, B.X. Ye, Food Chem. **129**, 1311 (2011)
41. C. Wang, R. Yuan, Y.Q. Chai, Y. Zhang, F.X. Hu, M.H. Zhang, Biosens. Bioelectron. **30**, 315 (2011)
42. A. Mohadesi, S. Parvaresh, Z. Eshaghi, M.A. Karimi, Electrochemistry **84**, 138 (2016)
43. S. William, J. Hummers, R.E. Offeman, J. Am. Chem. Soc. **80**, 1339 (1958)
44. H.P. Mungse, S. Verma, N. Kumar, B. Sain, O.P. Khatri, J. Mater. Chem. **22**, 5427 (2012)
45. I. Novak, M. Seruga, S. Komorsky-Lovric, Electroanalysis **21**, 1019 (2009)
46. M. Kahl, T.D. Golden, Electroanalysis **26**, 1664 (2014)